

Neural Network Method for Controlling the Helicopters Turboshaft Engines Free Turbine Speed at Flight Modes

Serhii Vladov, Yurii Shmelov, Ruslan Yakovliev, Yurii Stushchanskyi, and Yurii Havryliuk

Kremenchuk Flight College of Kharkiv National University of Internal Affairs, Peremohy street, 17/6, Kremenchuk, Poltavaska Oblast, Ukraine, 39605

Abstract

The work is devoted to the development of a method for controlling the main rotor speed, which is a key task to be solved in a helicopter flight. A modified block diagram of the circuit for maintaining the helicopters turboshaft engines free turbine speed an electronic PID-controller with a neural network tuning of the amplification factor has been developed, which made it possible to automatically adjust the amplification factor and, thereby, reduce the time of the transition process. The use of a dynamic neural network of direct data transmission based on neurons with a radial-basis activation function in the first layer and adalines – neurons with a linear activation function in the second layer is proposed, which made it possible to improve the quality of the transient process in terms of helicopters turboshaft engines turbine rotation frequency, which consists in an increase in performance up to 3 seconds, an increase in statistical accuracy up to $\pm 0.05\%$ and the elimination of parameter overshoot. The use of a dynamic neural network of direct data transmission as some functional converter that generates for a set of input and output signals the amplifications factors of the PID-controller made it possible to improve the probability of errors of the 1st and 2nd kind in comparison with the known controllers by 35... 85 %.

Keywords

Helicopters turboshaft engines, free turbine speed, neural network, training, PID-controller, transient processes, amplification factor, error

1. Introduction

The helicopters turboshaft engines (TE) are a complex thermogas-dynamic system with many features that must be taken into account when designing an automatic control system (ACS). The ACS of a modern aircraft engine performs many functions. These functions are distributed and carried out by a digital controller and hydromechanical actuators. The digital controller performs the main part of the engine control functions. Its main tasks are to control the TE operating modes, maintaining and/or limiting its various parameters, diagnosing and monitoring the state of the TE and ACS elements, and providing service and information functions. The task of the hydromechanical part of the ACS includes the control of the engine mechanization by the commands of the digital controller and the control of the operation of the gas turbine engine according to simplified laws in the event of an electronic system failure [1, 2].

The quality of control of TE parameters largely depends on the quality of tuning of electronic algorithms. Often in electronic control systems of TE linear controllers of P-, PD-, PI- and PID-type are used. Their popularity is explained by the simplicity of the mathematical description, low cost of implementation and sufficient efficiency. However, as practice shows, within the framework of the linear theory, it is not always possible to tune the PID-controller to ensure the required quality of

MoMLeT+DS 2023: 5th International Workshop on Modern Machine Learning Technologies and Data Science, June 3, 2023, Lviv, Ukraine.
EMAIL: ser26101968@gmail.com (S. Vladov); nviddil.klk@gmail.com (Yu. Shmelov); ateu.nv.klk@gmail.com (R. Yakovliev); skety@ukr.net (Yu. Stushchanskyi); gavriluk.sp@gmail.com (Yu. Havryliuk)
ORCID: 0000-0001-8009-5254 (S. Vladov); 0000-0002-3942-2003 (Yu. Shmelov); 0000-0002-3788-2583 (R. Yakovliev); 0000-0002-3021-6756 (Yu. Stushchanskyi); 0000-0002-5422-8161 (Yu. Havryliuk)



© 2023 Copyright for this paper by its authors.
Use permitted under Creative Commons License Attribution 4.0 International (CC BY 4.0).
CEUR Workshop Proceedings (CEUR-WS.org)

transients in a nonlinear system [3, 4], which are helicopters TE. Under these conditions, the use of neural network technologies is relevant and promising.

2. Related Works

When controlling complex non-linear objects, such as a helicopters TE, such controllers cannot always provide the required quality of control over TE parameters, stability and robustness of the system under changing operating conditions and failures. In this case, it makes sense to use alternative nonlinear controllers [5, 6]. For example, it can be a fuzzy logic controller (FLR), which has the property of robustness [7, 8]. Due to the absence of the need for a strict mathematical description of the object, logic controllers have gained great popularity among developers of electronic systems [9, 10]. The fuzzy control law obtained as a result of synthesis is non-linear and works well in systems with a high degree of complexity, non-linearities such as a dead zone, hysteresis, when the parameters of the unchanging part of the system deviate from their nominal values and information is lost in case of failures [11, 12]. It is worth noting that Elizaveta Chicherova conducted a number of alternative control methods research that make it possible to increase the stability margins of gas turbine engines ACS and eliminate oscillations using the following controllers: a linear PD controller with a reduced proportional gain, a square-law controller, a variable gain controller, a proportional fuzzy logic controller, a fuzzy logic controller with a proportional gain and a corrective differential link [13, 14], which made it possible to ensure the aperiodic nature of the transient process, to achieve a statistical accuracy of $\pm 0.2\%$ and a speed of up to 6 seconds.

However, when using these types of controllers, the overshoot value ranges from 0.1 to 2.2%. In order to eliminate overcasting, increase statistical accuracy and develop a method for controlling the speed of the free turbine of helicopters TE using neural network technologies, this is an urgent scientific and practical task.

3. Methods and Materials

The main task of the automatic control system of helicopters TE is to maintain the rotational speed of the main rotor n_{ng} . This task is accomplished by controlling the free turbine speed n_{FT} through the required fuel flow rate G_T . The value of the required fuel consumption is formed from the gas generator rotor r.p.m. n_{TC} and its derivative n_{TC_req} . Depending on the engine operating mode, the value of the required derivative of the gas generator rotor r.p.m. is formed by various circuits. For example, in idle mode, the value of n_{TC_req} is determined by the circuit for maintaining the required speed of the turbocharger rotor, and at flight mode, by the circuit for maintaining the free turbine speed. Since the helicopter TE can be operated at flight mode for a significant part of the time, the choice of the structure and parameters of the electronic controller determines the dynamic quality of helicopter TE control and its resource.

The mathematical model of the regulated object – the helicopter TE (in this work, the deviations of the state variables are considered) according to [15] has the form:

$$\begin{aligned} \tau_1 \frac{dn_{TC}}{dt} + n_{TC} &= k_{11} G_T; \\ \tau_2 \frac{dn_{FT}}{dt} + n_{FT} &= k_{21} G_T + k_{22} n_{TC}; \end{aligned} \quad (1)$$

where G_T – fuel consumption, τ_1 and τ_2 – time constants, k_{11} , k_{21} , k_{22} – amplification factors.

The analysis of the object of regulation – the helicopter TE according to [15] is presented in the form of a series connection of dynamic links with transfer functions:

$$\begin{aligned} W_{TC} &= \frac{n_{TC}}{G_T} = \frac{k_{11}}{\tau_1 p + 1}; \\ W_{FT} &= \frac{n_{FT}}{n_{TC}} = \left(1 + \frac{k_{21}}{k_{22} W_{TC}} \right) \cdot \left(\frac{k_{22}}{\tau_2 p + 1} \right). \end{aligned} \quad (2)$$

The mathematical model of the fuel dispenser with a direct drive from an electromechanical converter according to [15, 16] after dry friction linearization is represented as:

$$J \frac{d^2 \alpha}{dt^2} + k_v \frac{d\alpha}{dt} = k_i \cdot i; \quad (3)$$

$$G_T = \alpha \cdot k_{G_T};$$

where J – rotor inertia moment, α – rotor rotation angle, k_v , k_i , k_{G_T} – coefficients of viscous friction, torque and fuel consumption, i – control current.

Thus, the transfer function of the fuel dispenser is presented in the following form [15]:

$$W_{FD} = \frac{k_i \cdot k_{G_T}}{p \cdot (J \cdot p + k_v)}. \quad (4)$$

For the internal fuel consumption control loop, a proportional-differential control law is adopted:

$$W_{PD} = \frac{i}{G_{T_{given}} - G_T} = k_P + k_D \cdot p; \quad (5)$$

where $G_{T_{given}}$ – fuel consumption setpoint, k_P and k_D – proportional and differential gains.

According to [15, 17], to take into account the delay of the digital control unit, a link of pure delay by $1.5 \cdot T$ is introduced, where T – sampling period in time:

$$W_{delay} = e^{-1.5 \cdot p \cdot T}; \quad (6)$$

at the same time, for the transfer function of a closed internal fuel consumption control loop, the following expression is obtained:

$$W_{G_T} = \frac{W_0}{1 + W_0}; \quad (7)$$

where $W_0 = W_{delay} \cdot W_{PD} \cdot W_{FD}$.

According to [15], as a control law n_{FT} , a proportional-integral control law with a transfer function is adopted:

$$W_{PI} = \frac{i}{n_{FT_{req}} - n_{FT}} = k_{P1} + \frac{k_i}{p}; \quad (8)$$

where $n_{FT_{req}}$ – set value of the free turbine speed, k_{P1} and k_i – gains of the proportional and integral components.

To exclude the sequential inclusion of two integral components for an additional internal control loop n_{TC} , a proportional control law is adopted:

$$W_P = \frac{G_{T_{set}}}{n_{TC_{set}} - n_{TC}} = k_{P2}; \quad (9)$$

where $n_{TC_{set}}$ – set value of the gas generator rotor r.p.m., k_{P2} – amplification factor.

According to [15], the value of the gain is chosen from the condition of ensuring the required accuracy of the implementation of the law $\frac{dn_{TC}}{dt} = f(U)$ in all modes of engine operation.

The transfer function of the open control loop n_{FT} with independent operation of the controller is presented in the following form:

$$W_1 = W_{PI} \cdot W_P \cdot W_{G_T} \cdot W_{TC} \cdot W_{FT}. \quad (10)$$

Similarly, the open-loop transfer function n_{FT} when operated in series with an n_{TC} controller is:

$$W_2 = W_1 \cdot W_4; \quad (11)$$

where

$$W_4 = \frac{1}{1 + W_P \cdot W_{G_T} \cdot W_{TC}}. \quad (12)$$

In connection with the foregoing, an improved typical circuit for maintaining the free turbine speed of helicopters TE with a linear PID controller is proposed (fig. 1).

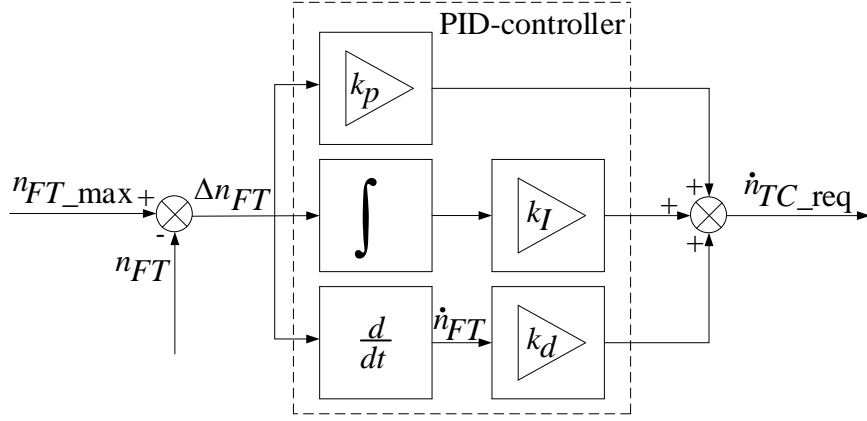


Figure 1: Modified block diagram of the circuit for maintaining of helicopters turboshaft engines free turbine speed with a linear electronic controller (developed based on [13, 14])

The error of the mismatch between the current and required value of the free turbine speed Δn_{FT} , and the derivative of the current free turbine speed \dot{n}_{FT} , is fed to the loop input, and the output signal is the value of the required derivative of the turbocharger rotor speed. The expression describing the circuit for maintaining the free turbine speed with a linear PID-controller has the form:

$$\dot{n}_{TC_req} = \Delta n_{FT} \cdot k_p + n_{FT} \cdot k_d. \quad (13)$$

The gains of the proportional k_p and differential k_d links are determined from the equations:

$$\begin{aligned} k_p &= k(\Delta n_{FT}) \cdot k_{stat_p} \cdot G_{T_stat}(n_{TC}) \cdot a_{13}(n_{TC}); \\ k_d &= k_{stat_d} \cdot \tau_{FT}(n_{TC}); \end{aligned} \quad (14)$$

where $G_{T_stat}(n_{TC})$ – characteristic of the static fuel consumption, $a_{13}(n_{TC})$ – coefficient of engine linear dynamic model in terms of fuel consumption, $\tau_{FT}(n_{TC})$ – time constant of the free turbine rotor.

The coefficient is given by the following system of equations:

$$k(\Delta n_{FT}) = \begin{cases} |\Delta n_{FT}|, & \text{if } \Delta n_{FT} \leq 1; \\ 1 + \frac{\Delta n_{FT} - 1}{2}, & \text{if } 1 < \Delta n_{FT} \leq 3; \\ \frac{2 \cdot (\Delta n_{FT} + 4)}{7}, & \text{if } \Delta n_{FT} > 3; \end{cases} \quad (15)$$

The static coefficient of the proportional link is $k_{stat_p} = 0.35$, while that of the differential link is $k_{stat_d} = 0.05$ [13, 14].

Since the main task solved in the helicopter flight mode is to maintain the main rotor speed, it is advisable to apply the neural network setting of the coefficients k_p , k_i and k_d , which will eventually allow dynamic maintenance of the main rotor speed.

It is assumed that, in general, the circuit for maintaining the speed of the free turbine of the gas turbine engine of helicopters with a linear electronic controller is described by the following equation:

$$\dot{X} = A(t)X + B(t)u + f(t); \quad (16)$$

where $x = (x_1 \dots x_n)^T$ – state vector of the system under the action of control $u = (u_1, u_2, u_3)^T$, – components of which are constants under the constraints $|u_i| < 1$, $i = 1, 2, 3$. The elements of the matrices $A(t)$, $B(t)$ and the vector $f(t)$ will be considered real, continuous functions for $t \in [0, T]$, their dimensions are $(n \times n)$, $(n \times 3)$ and $(n \times 1)$, respectively. The matrix $B(t)$ is determined by a predetermined real and

continuous at $t \in [0, T]$ vector $b(t) = \begin{pmatrix} b_1(t) \\ \dots \\ b_n(t) \end{pmatrix}$ in the form:

$$B(t) = \left(b(t), \int_0^t b(\tau) d\tau, \dot{b}(t) \right). \quad (17)$$

To obtain an equation describing the search for the coefficients k_p , k_i and k_d , under which the quality of the control system will be the best or will satisfy the specified requirements, the assumptions are made that $k_p = \text{const}$, $k_i = \text{const}$ and $k_d = \text{const}$. It is assumed that the vector function $b(t)$ satisfies the inequality $a_1 e^{-\lambda t} \leq \|b(t)\| \leq a_2 e^{-\lambda t}$ for some positive λ and $a_1 < a_2$. Then, due to the choice of control u , it is necessary to achieve exponential stability of the original system. It is accepted that

$$b(t) = B_1(t); \int_0^t b(\tau) d\tau = B_2(t); \dot{b}(t) = B_3(t); \quad (18)$$

where the vectors $B_1(t)$, $B_2(t)$, $B_3(t)$ make up the matrix $B(t)$.

Initially, the coefficients u , considered as control, are assumed to be constant. However, for further research, a new control $\bar{u}(t)$ is introduced, which will be a function of time, that is,

$$u = \bar{u}(t)x. \quad (19)$$

In order for the program motion $x(t, \bar{u}(t))$ together with the control $\bar{u}(t)$ to set the product constant $\bar{u}(t)x(t, \bar{u}(t))$, system (16) is represented as:

$$\dot{x} = \left(A(t) + \sum_{i=1}^3 B_i(t) \bar{u}_i(t) \right) x + f(t). \quad (20)$$

Let be $Z(t, \bar{u})$ – matrix of the fundamental system of solutions corresponding to the homogeneous system (20) for $f(t) \equiv 0$. Then for $Z(t, \bar{u})$ will be fulfilled

$$\dot{Z}(t, \bar{u}) = \left(A(t) + \sum_{i=1}^3 B_i(t) \bar{u}_i(t) \right) Z(t, \bar{u}); \quad (21)$$

in this case, $Z^{-1}(t, \bar{u})$ – inverse matrix $Z(t, \bar{u})$.

It follows that the general solution in the Cauchy form of system (21) with initial data $x_0 = x(0)$ will be written in the form:

$$x(t, \bar{u}) = Z(t, \bar{u})x_0 + Z(t, \bar{u}) \int_0^t Z^{-1}(\tau, \bar{u}) f(\tau) d\tau. \quad (22)$$

It should be noted that the choice of control is subject to restrictions caused by the operating conditions of helicopters TE at flight mode. Therefore, it is necessary to take into account this possibility and add admissibility conditions for the values of the coefficients:

$$\int_0^T \sum_{i=1}^3 \bar{u}_i^{-2}(t) dt \leq \varphi; \quad (23)$$

where φ – positive constant, T – length of the time interval on which the program control law will operate in the form of fixed coefficients $\bar{u}(t)$. Let's introduce the following functional:

$$J(\bar{u}) = \bar{u}(t) = x^2(t, \bar{u}); \quad (24)$$

where $x(t, \bar{u})$ – solution of the Cauchy task (22) determined by the functional law of coefficients $\bar{u}(t)$ during the time interval $[0, T]$.

Let us assume that there is an optimal control [18, 19] in the form $\bar{u}^{(0)} = \left(\bar{u}_1^{(0)}(t), \bar{u}_2^{(0)}(t), \bar{u}_3^{(0)}(t) \right)^T$ that gives the functional (24) the minimum possible value, while simultaneously fulfilling the condition:

$$\int_0^T \sum_{i=1}^3 \left(\bar{u}_i^{(0)}(t) \right)^2 dt = \varphi. \quad (25)$$

Then any other control from some local proximity to the optimal will have the form:

$$\bar{u} = \bar{u}^{(0)} + \varepsilon v = \left(\bar{u}_1^{(0)}(t) + \varepsilon v_1(t), \bar{u}_2^{(0)}(t) + \varepsilon v_2(t), \bar{u}_3^{(0)}(t) + \varepsilon v_3(t) \right)^T; \quad (26)$$

and the admissibility condition must also be satisfied for it, but the inequality will necessarily be true:

$$J\left(\bar{u}^{(-0)}\right) = J\left(\bar{u}^{(-0)} + \varepsilon v\right) \quad (27)$$

for all sufficiently small ε . Then, taking into account the individual choice, a vector function $v(t)$ is accepted that satisfies the requirement

$$\int_0^T \sum_{i=1}^3 v_i(t) \bar{u}_i^{(-0)}(t) dt \neq 0 \quad (28)$$

and, therefore, under the admissibility condition for non-optimal control $\bar{u} = \bar{u}^{(-0)} + \varepsilon v$ and taking into account the square under the integral sign in this condition, we notice that $\text{sign} \varepsilon = -\text{sign} \int_0^T \sum_{i=1}^3 v_i(t) \bar{u}_i^{(-0)}(t) dt$. From the need to minimize the functional $J\left(\bar{u}^{(-0)} + \varepsilon v\right)$ for the value of the parameter $\varepsilon = 0$, the following inequalities will necessarily hold:

$$\begin{aligned} \frac{dJ}{d\varepsilon} &\geq 0 \text{ for } \varepsilon > 0 \text{ or } \int_0^T \sum_{i=1}^3 v_i(t) \bar{u}_i^{(-0)}(t) dt < 0; \\ \frac{dJ}{d\varepsilon} &\leq 0 \text{ for } \varepsilon < 0 \text{ or } \int_0^T \sum_{i=1}^3 v_i(t) \bar{u}_i^{(-0)}(t) dt > 0. \end{aligned} \quad (29)$$

It is assumed that the structure of the derivative of the functional $J(u)$ has the form

$$\frac{dJ\left(\bar{u}^{(-0)} + \varepsilon v\right)}{d\varepsilon} = \int_0^T \sum_{i=1}^3 \psi_i\left(\bar{u}^{(-0)}\right) v_i(t) dt; \quad (30)$$

where $\psi_i\left(\bar{u}^{(-0)}\right)$ – functions, but depending on the optimal control and on the right-hand sides of system (20).

If we assume that $\bar{u}_1^{(-0)}(t) \equiv 0$, but at the same time assume that the controls $v_2(t) = v_3(t) = 0$ and $v_1(t) = \alpha \cdot \bar{u}_1^{(-0)}(t) + \omega(t)$, where is a constant $\alpha = \frac{\int_0^T v_1(t) \bar{u}_1^{(-0)}(t) dt}{\int_0^T \left(\bar{u}_1^{(-0)}(t)\right)^2 dt}$, then by direct substitution into (28)

we obtain that $\int_0^T \bar{u}_1^{(-0)}(t) \omega(t) dt$, that is, the function $\omega(t)$ will be orthogonal to $\bar{u}_1^{(-0)}(t)$. Noting that for each control of the form $v_1(t) = \alpha \bar{u}_1^{(-0)}(t) + \beta \omega(t)$ for any β , we find that any of the inequalities (29), taking into account the choice of the structure in the form (30), for a sufficiently large modulo value of the parameter β will be violated:

$$\int_0^T \sum_{i=1}^3 \psi_i(t) v_i(t) dt = \int_0^T \psi_1(t) v_1(t) dt = \beta \int_0^T \psi_1(t) \omega(t) dt + \alpha \int_0^T \psi_1(t) \bar{u}_1^{(-0)}(t) dt < 0; \quad (31)$$

but it can only be done under one condition:

$$\int_0^T \psi_1(t) \omega(t) dt = 0. \quad (32)$$

The resulting expressions show that the function $\psi_1(t)$ is orthogonal to any function orthogonal to $\bar{u}_1^{(-0)}(t)$, that is, we can assume that $\psi_1 = \alpha_1 \cdot \bar{u}_1^{(-0)}(t)$. Similarly, $\psi_i = \alpha_i \cdot \bar{u}_i^{(-0)}(t)$ for some constants α_i , $i = 1, 2, 3$. Let us express the optimal control $\bar{u}^{(-0)}$ from these equations in the form

$$\bar{u}_i^{(-0)}(t) = \beta_i \cdot \psi_i(t); \quad (33)$$

where constants $\beta_i = \frac{\int_0^T \bar{u}_i^{(-0)}(t) \psi_i(t) dt}{\int_0^T \psi_i^2(t) dt}$, $i = 1, 2, 3$.

The resulting expression (33) is a consequence of relations (29) and, in essence, represent the necessary conditions for the optimality of controls $\bar{u}_1^{(0)}(t)$, $\bar{u}_2^{(0)}(t)$, $\bar{u}_3^{(0)}(t)$ on the time interval $[0, T]$.

Let us now formulate the general principle of actually finding the functions $\psi_i\left(\bar{u}^{(0)}(t)\right)$, which determine the method of software adjustment of the gains $\bar{u}^{(0)}$ according to expression (33). Let us first

find the derivative of the functional $\frac{dJ\left(\bar{u}^{(0)} + \varepsilon v\right)}{d\varepsilon}$ at $\varepsilon = 0$ and time $t = T$. To do this, using the general solution formula in the Cauchy form, we first derive:

$$\begin{aligned} \frac{dx\left(T, \bar{u}^{(0)} + \varepsilon v\right)}{d\varepsilon} &= x_0 \frac{dZ\left(T, \bar{u}^{(0)} + \varepsilon v\right)}{d\varepsilon} + \frac{dZ\left(T, \bar{u}^{(0)} + \varepsilon v\right)}{d\varepsilon} \cdot \int_0^T Z^{-1}\left(t, \bar{u}^{(0)} + \varepsilon v\right) f(t) dt + Z\left(T, \bar{u}^{(0)} + \varepsilon v\right) \times \\ &\times \int_0^T \frac{dZ^{-1}\left(t, \bar{u}^{(0)} + \varepsilon v\right)}{d\varepsilon} f(t) dt = x_0 Z\left(T, \bar{u}^{(0)} + \varepsilon v\right) \cdot \int_0^T B_i(t) v_i(t) dt + Z\left(T, \bar{u}^{(0)} + \varepsilon v\right) \cdot \int_0^T \sum_{i=1}^3 B_i(t) v_i(t) dt \times \\ &\times \int_0^T Z^{-1}\left(t, \bar{u}^{(0)} + \varepsilon v\right) f(t) dt - Z\left(T, \bar{u}^{(0)} + \varepsilon v\right) \cdot \int_0^T Z^{-1}\left(t, \bar{u}^{(0)} + \varepsilon v\right) f(t) dt \cdot \int_0^t \sum_{i=1}^3 B_i(\tau) v_i(\tau) d\tau f(t) dt = \\ &= x_0 Z\left(T, \bar{u}^{(0)} + \varepsilon v\right) \cdot \int_0^T B_i(t) v_i(t) dt + Z\left(T, \bar{u}^{(0)} + \varepsilon v\right) \cdot \int_0^T \sum_{i=1}^3 B_i(t) v_i(t) dt \cdot \int_0^T Z^{-1}\left(t, \bar{u}^{(0)} + \varepsilon v\right) f(t) dt - \\ &- Z\left(T, \bar{u}^{(0)} + \varepsilon v\right) \cdot \int_0^t \sum_{i=1}^3 B_i(\tau) v_i(\tau) d\tau d\left(\int_0^t Z^{-1}\left(\tau, \bar{u}^{(0)} + \varepsilon v\right) f(\tau) d\tau\right) = x_0 Z\left(T, \bar{u}^{(0)} + \varepsilon v\right) \cdot \int_0^T B_i(t) v_i(t) dt + \\ &+ Z\left(T, \bar{u}^{(0)} + \varepsilon v\right) \cdot \int_0^T \int_0^t Z\left(\tau, \bar{u}^{(0)} + \varepsilon v\right) f(\tau) d\tau \cdot \sum_{i=1}^3 B_i(t) v_i(t) dt. \end{aligned} \quad (34)$$

Then, assuming the moment of time $t = T$, we find

$$\begin{aligned} \left. \frac{dJ\left(\bar{u}^{(0)} + \varepsilon v\right)}{d\varepsilon} \right|_{\varepsilon=0} &= 2x\left(T, \bar{u}^{(0)}\right) \left. \frac{dx\left(T, \bar{u}^{(0)} + \varepsilon v\right)}{d\varepsilon} \right|_{\varepsilon=0} = 2 \cdot \left(x_0 Z\left(T, \bar{u}^{(0)}\right) + Z\left(T, \bar{u}^{(0)}\right) \int_0^T Z^{-1}\left(T, \bar{u}^{(0)}\right) f(t) dt \right) \times \\ &\times \left(x_0 Z\left(T, \bar{u}^{(0)}\right) \int_0^T \sum_{i=1}^3 B_i(t) v_i(t) dt + Z\left(T, \bar{u}^{(0)}\right) \cdot \int_0^T \int_0^t Z\left(\tau, \bar{u}^{(0)}\right) f(\tau) d\tau \cdot \sum_{i=1}^3 B_i(t) v_i(t) dt \right) = \\ &= \int_0^T \sum_{i=1}^3 \psi_i\left(t, \bar{u}^{(0)}\right) v_i(t) dt; \end{aligned} \quad (35)$$

where

$$\begin{aligned} \psi_i\left(t, \bar{u}^{(0)}\right) &= 2 \cdot \left(Z\left(T, \bar{u}^{(0)}\right) x_0 + Z\left(T, \bar{u}^{(0)}\right) \cdot \int_0^T Z^{-1}\left(\tau, \bar{u}^{(0)}\right) f(\tau) d\tau \right) \cdot \left(Z\left(T, \bar{u}^{(0)}\right) x_0 + Z\left(T, \bar{u}^{(0)}\right) \times \right. \\ &\left. \times \int_0^T Z^{-1}\left(\tau, \bar{u}^{(0)}\right) f(\tau) d\tau \right) B_i(t). \end{aligned} \quad (36)$$

It can be seen from (36) that the functions $\psi_i\left(t, \bar{u}^{(0)}\right)$ depend on the index i only through the corresponding function $B_i(t)$. Thus, having determined the type of functions $\psi_i\left(t, \bar{u}^{(0)}\right)$ through the dependence on the optimal control $\bar{u}^{(0)}$ and the type of system (20), in the future, an algorithm for programmatic adjustment of the gains and will be proposed, which will play the role of a “teacher”

4. Experiment

On a cycle, the neural network receives the setpoint and generates the control coefficients of the PID-controller, which are fed to the PID-controller along with the value of the current feedback error $e(k)$. The PID-controller calculates the control signal according to the expression:

$$u(k) = u(k-1)u_1(k)(e(k) - e(k-1)) + u_2(k)e(k) + u_3(k)(e(k) - 2e(k-1) + e(k-2)); \quad (37)$$

used for discrete PID-controllers and feeds it to the control object – the helicopters TE. The neural network is trained in real time by feedback error.

Let the entire observation time be divided into time intervals of length T : $[0, T]$, $[0, 2T]$, $[2T, 3T]$, ... Within each individual segment $[sT, (s+1)T]$, $s = 0, 1, 2, \dots$ is used as a “teacher” for a neural network, the method of programmatic adjustment of gain factors, described in this paper.

When synthesizing the controller, a dynamic network of direct data transmission was used, based on neurons with a radial basis activation function in the first layer and adalines – neurons with a linear activation function, in the second layer. At the same time, on test examples, the optimal settings of the neural network were obtained, which provide the smallest overshoot for a given time of the transient process [20]. The following sequences are used as neuroregulator inputs:

- reference signal – a master sequence that determines the final state of the object,
- controller output – feedback from the controller output,
- object error – the difference between the reference signal and the real output of the object,
- integrable error – the error accumulated by the controller for the entire time of the object operation,
- object output – signal from the object output.

The choice of input sequences is not random. Some of the sequences are intended only for a certain component of the control signal. So, the output of the object and the output of the controller are necessary for the differential component and the adjustment of the parameters of the predictor, which actually implements the differentiation function. The “integrable error” sequence is only necessary for the integral component and affects only it. The remaining incoming sequences affect all neurons of each of the blocks (fig. 2).

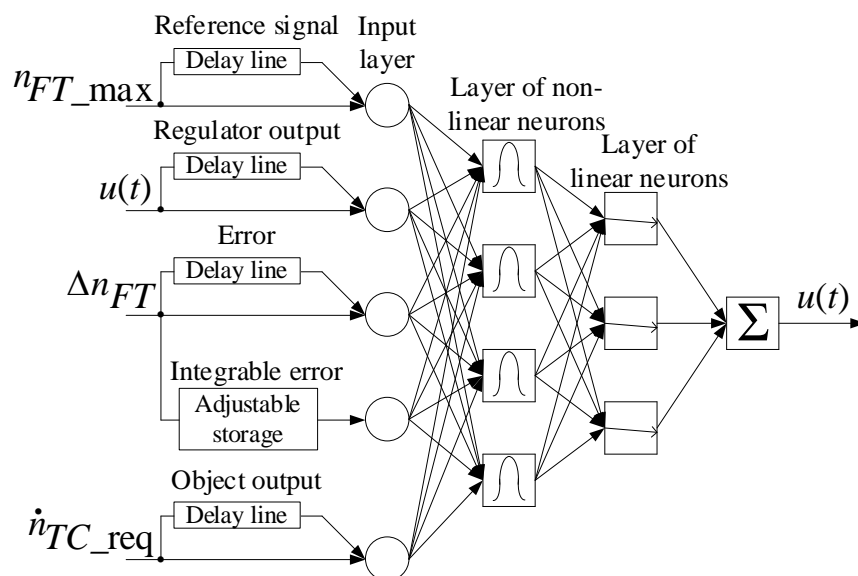


Figure 2: Neural network diagram (developed based on [20])

The ACS structure, which includes a neural network in the role of setting the coefficients, using a PID controller, is schematically shown in fig. 3 (developed on the basis of [21]), in which the neural network plays the role of some functional converter that generates the required coefficients of the PID controller k_p , k_i , k_d for a set of signals n_{FT_max} , Δn_{FT} , u , \dot{n}_{TC_req} .

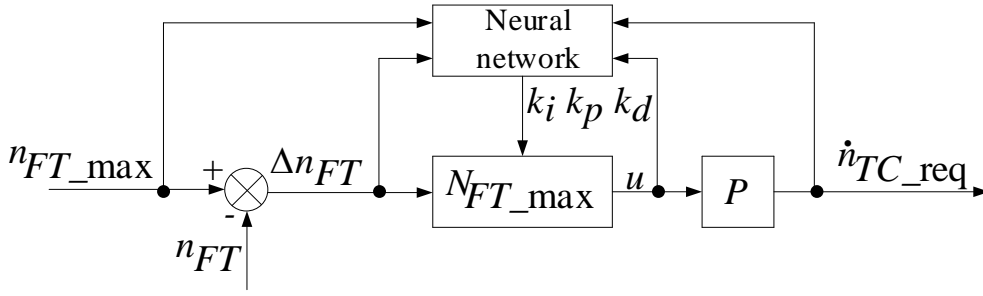


Figure 3: PID-controller structure with auto-tuning block based on a neural network (developed based on [21])

Let us consider a method for approximate construction of an optimal control based on the application of (33) and assume that

$$\bar{u}_i^{-(l+1)} = \alpha \left(\bar{u}^{-(l)} \right) \beta_i \left(\bar{u}^{-(l)} \right) \psi_i \left(\bar{u}^{-(l)} \right); \quad (38)$$

where $\bar{u}^{-(l)} = \left(\bar{u}_1^{-(l)}, \bar{u}_2^{-(l)}, \bar{u}_3^{-(l)} \right)$ – l -th successive approximation, and the constant factors β have the form

$$\beta_i \left(\bar{u}^{-(l)} \right) = \frac{\int_0^T \bar{u}^{-(l)}(t) \psi_i \left(t, \bar{u}^{-(l)} \right) dt}{\int_0^T \psi_i^2 \left(t, \bar{u}^{-(l)} \right) dt}. \text{ The value } \alpha \left(\bar{u}^{-(l)} \right) \text{ is chosen so that } \int_0^T \sum_{i=1}^3 \left(\bar{u}_i^{-(l+1)}(t) \right)^2 dt = \varphi, \text{ that is}$$

$$\int_0^T \sum_{i=1}^3 \left(\bar{u}_i^{-(l+1)}(t) \right)^2 dt = \sum_{i=1}^3 \int_0^T \left(\bar{u}_i^{-(l+1)}(t) \right)^2 dt = \alpha^2 \left(\bar{u}^{-(l)} \right) \sum_{i=1}^3 \frac{\left(\int_0^T \bar{u}^{-(l)}(t) \psi_i \left(t, \bar{u}^{-(l)} \right) dt \right)^2}{\left(\int_0^T \psi_i^2 \left(t, \bar{u}^{-(l)} \right) dt \right)^2} \int_0^T \psi_i^2 \left(t, \bar{u}^{-(l)} \right) dt = \alpha^2 \left(\bar{u}^{-(l)} \right) \times$$

$$= \alpha^2 \left(\bar{u}^{-(l)} \right) \frac{\sum_{i=1}^3 \left(\int_0^T \bar{u}^{-(l)}(t) \psi_i \left(t, \bar{u}^{-(l)} \right) dt \right)^2}{\sum_{i=1}^3 \int_0^T \psi_i^2 \left(t, \bar{u}^{-(l)} \right) dt}. \text{ Thus, } \alpha \left(\bar{u}^{-(l)} \right) = \sqrt{k \left(\frac{\sum_{i=1}^3 \left(\int_0^T \bar{u}^{-(l)}(t) \psi_i \left(t, \bar{u}^{-(l)} \right) dt \right)^2}{\sum_{i=1}^3 \int_0^T \psi_i^2 \left(t, \bar{u}^{-(l)} \right) dt} \right)^{-1}}.$$

Thus, following [21], a sequence is constructed that approximates the optimal control $\bar{u}^{-(l)}$ for the entire observation interval $[0, T]$. Note that in [21] it is not indicated at which step in the construction of an approximate control to stop one's choice. Having fixed some approximate control $\bar{u}^{-(l)}(t)$, we obtain a time-varying control (in this problem, the time-varying $[0, T]$ coefficients of the PID-controller). However, this control will be deprived of the possibility of correction if the value of the control error is exceeded, caused, for example, by fixing an insufficiently large approximation step or by the presence of an unexpected random perturbation of the function $f(t)$ (although it is considered deterministic).

It is assumed that the time T is not the entire observation time of the controlled dynamic process, but only its rather small segment of the algorithmic stepwise sampling (not the time sampling step used in the calculations), that is, the entire observation time will be divided into time segments of length T : $[0, T]$, $[0, 2T]$, $[2T, 3T]$, ... Within each individual segment $[sT, (s+1)T]$, $s = 0, 1, 2, \dots$, we will apply the method of software adjustment of gain coefficients.

As a first approximation $\bar{u}^{-(1,s)}$, we take the constant values $\bar{u}^{-(2,s+1)}(sT)$ obtained at the previous step of the algorithm with the help of control $\bar{u}^{-(2,s+1)}(sT)$ at the time sT of the corresponding time interval of the algorithmic discredit $[(s-1)T, sT]$. In this case, the initial point x_0 from (22) will also be given

by the value $x\left(sT, \bar{u}^{-(2,s+1)}\right)$ obtained at the boundary time. Thus, at this stage, we define the following approximation:

$$\bar{u}_i^{-(2,s)}(t) = \alpha\left(\bar{u}^{-(2,s+1)}(sT)\right)\beta_i\left(\bar{u}^{-(2,s+1)}(sT)\right)\psi_i\left(t, \bar{u}^{-(2,s+1)}(sT)\right); \quad (39)$$

where the functions $\psi_i\left(t, \bar{u}^{-(2,s+1)}(sT)\right)$, $i = 1, 2, 3$ are found by expressions (36), taking into account the time shift $t = t + sT$ for all functions included in this expression:

$$\begin{aligned} \psi_i\left(t, \bar{u}^{-(2,s+1)}(sT)\right) &= 2x\left(sT, \bar{u}^{-(2,s-1)}(sT)\right)Z\left((s+1)T, \bar{u}^{-(2,s+1)}(sT)\right) + Z\left((s+1)T, \bar{u}^{-(2,s-1)}(sT)\right) \times \\ &\times \int_{sT}^{(s+1)T} Z^{-1}\left(\tau, \bar{u}^{-(2,s-1)}(sT)\right), f(\tau) d\tau \cdot \left(x\left(sT, \bar{u}^{-(2,s-1)}(sT)\right)Z\left((s+1)T, \bar{u}^{-(2,s-1)}(sT)\right) + Z\left((s+1)T, \bar{u}^{-(2,s-1)}(sT)\right) \times \right. \\ &\quad \left. \times \int_{sT}^{(s+1)T} Z^{-1}\left(\tau, \bar{u}^{-(2,s-1)}(sT)\right), f(\tau) d\tau \right) B_i(t). \end{aligned} \quad (40)$$

Thus, we obtain the final expressions for determining α and β_i :

$$\alpha\left(\bar{u}^{-(2,s-1)}(sT)\right) = \sqrt{\varphi \cdot \left(\frac{\sum_{i=1}^3 \left(\int_0^{(s+1)T} \bar{u}^{-(2,s-1)}(sT) \psi_i\left(t, \bar{u}^{-(2,s-1)}(sT)\right) dt \right)^2}{\int_0^{(s+1)T} \psi_i^2\left(t, \bar{u}^{-(2,s-1)}(sT)\right) dt} \right)^{-1}}; \quad (41)$$

$$\beta_i\left(\bar{u}^{-(2,s-1)}(sT)\right) = \frac{\int_0^{(s+1)T} \bar{u}^{-(2,s-1)}(sT) \psi_i\left(t, \bar{u}^{-(2,s-1)}(sT)\right) dt}{\int_0^{(s+1)T} \psi_i^2\left(t, \bar{u}^{-(2,s-1)}(sT)\right) dt}. \quad (42)$$

The input parameters of helicopters TE mathematical model are the values of atmospheric parameters (h – flight altitude, T_N – temperature, P_N – pressure, ρ – air density). The parameters recorded on board of the helicopter (n_{FT} – free turbine rotor speed) reduced to absolute values according to the theory of gas-dynamic similarity developed by Professor Valery Avgustinovich (table 1). We assume in the work that the atmospheric parameters are constant (h – flight altitude, T_N – temperature, P_N – pressure, ρ – air density) [22].

Table 1

Fragment of the training sample

Number	n_{FT}	Number	n_{FT}
1	0.943	8	0.969
2	0.982	9	0.947
3	0.962	10	0.953
4	0.987	11	0.955
5	0.972	12	0.959
6	0.963
7	0.962	256	0.981

To form the training and test subsets, cross-validation [23] was used to estimate the values of n_{FT} , the results of which are shown in fig. 4.

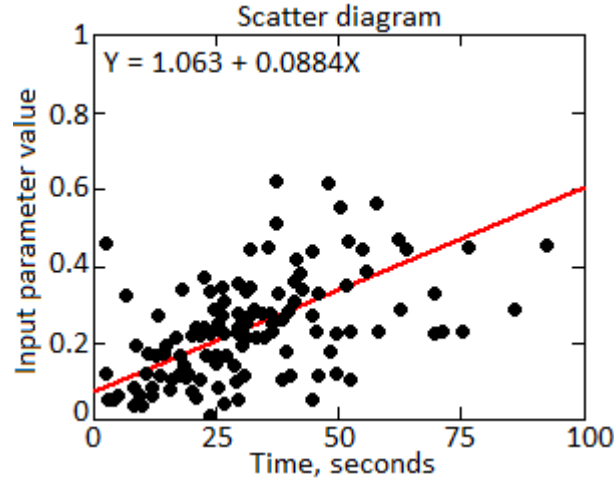


Figure 4: Scatter diagram of input parameters

In order to establish the representativeness of the training and test samples, a cluster analysis [22, 24] of the initial data was carried out (table 1), during which seven classes were identified (fig. 5, a). After the randomization procedure, the actual training (control) and test samples were selected (in a ratio of 2:1, that is, 67% and 33%). The process of clustering the training (fig. 5, b) and test samples shows that they, like the original sample, contain seven classes each. The distances between the clusters practically coincide in each of the considered samples, therefore, the training and test samples are representative.

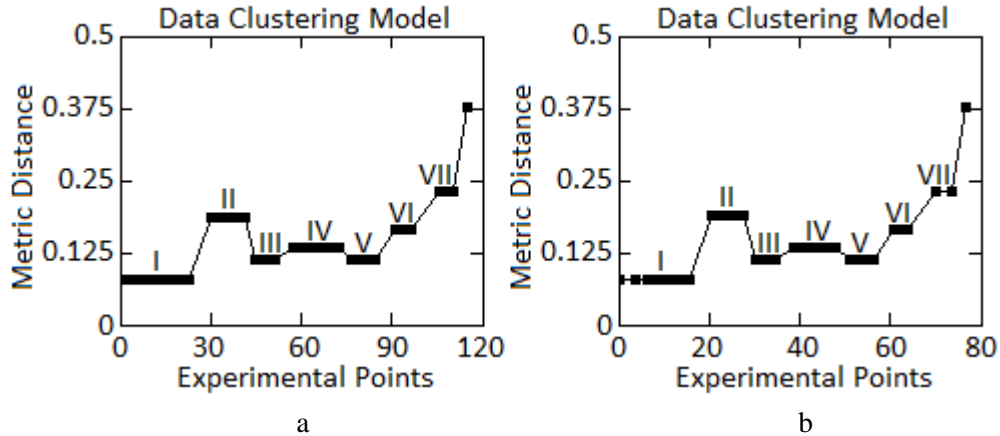


Figure 5: Clustering results: a – initial experimental sample (I...VII – classes); b – training sample

An important issue is the assessment of the homogeneity of the training and test samples. To do this, we use the Fisher-Pearson criterion χ^2 [22, 25] with $r - k - 1$ degrees of freedom:

$$\chi^2 = \min_{\theta} \sum_{i=1}^r \left(\frac{m_i - np_i(\theta)}{np_i(\theta)} \right)^2; \quad (43)$$

where θ – maximum likelihood estimate found from the frequencies m_1, \dots, m_r ; n – number of elements in the sample; $p_i(\theta)$ – probabilities of elementary outcomes up to some indeterminate k -dimensional parameter θ .

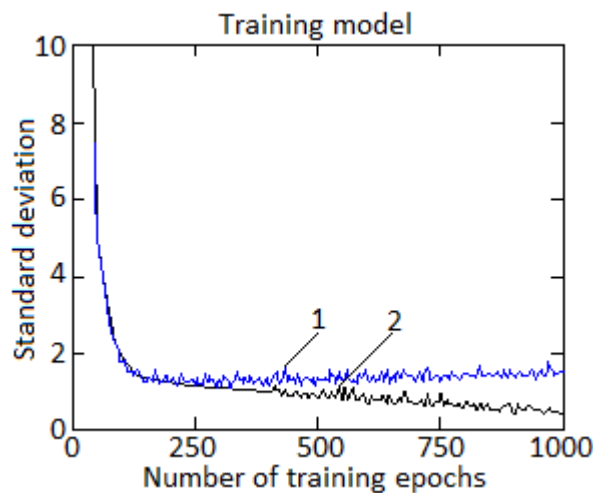
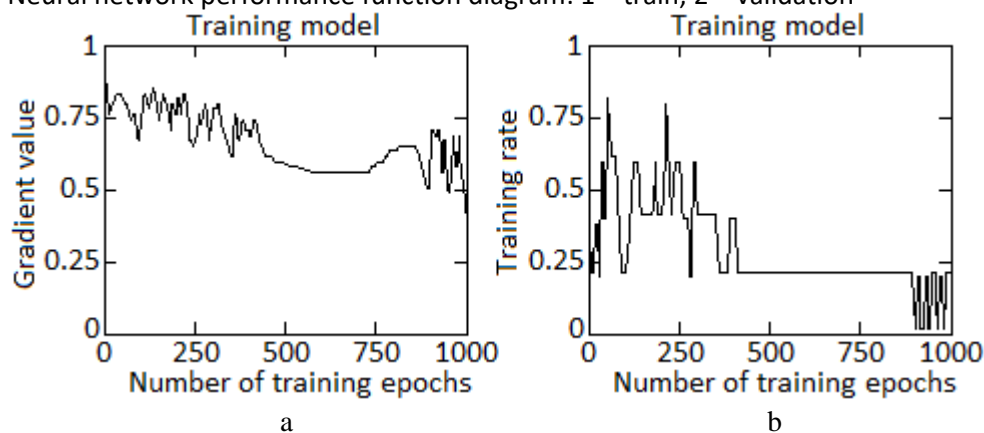
The specified statistics χ^2 allows, under the above assumptions, to test the hypothesis about the representability of sample variances and covariances of factors contained in the statistical model. The area of acceptance of the hypothesis is $\chi^2 \leq \chi_{n-m, \alpha}^2$, where α – significance level of the criterion. The results of calculations according to (43) are given in table 2.

Table 2Fragment of χ^2 probabilities

Number	$P(n_{FT})$	Number	$P(n_{FT})$
1	0.652	8	0.971
2	0.574	9	0.658
3	0.515	10	0.663
4	0.655	11	0.664
5	0.612	12	0.588
6	0.515
7	0.515	256	0.651

Calculating the value of χ^2 from the observed frequencies m_1, \dots, m_r (summing line by line the probabilities of the outcomes of each measured value) and comparing it with the critical values of the distribution χ^2 with the number of degrees of freedom $r - k - 1$. In this work, with the number of degrees of freedom $r - k - 1 = 13$ and $\alpha = 0.05$, the random variable $\chi^2 = 0.687$ did not exceed the critical value from table 2 is 22.362, which means that the hypothesis of the normal distribution law can be accepted and the samples are homogeneous.

The neural network was trained by the above method for 1000 epochs, the training accuracy characteristic is shown in fig. 6, the steady-state mean square error is 0.382. Fig. 7 shows the results of the neural network training validation test, from which it can be seen that the average value of the gradient is, and the optimal value of the training coefficient does not exceed 1.

**Figure 6:** Neural network performance function diagram: 1 – train; 2 – validation**Figure 7:** Neural network training diagram: a – gradient change diagram; b – diagram of the change in the training coefficient of the neural network

The circuit for maintaining of helicopters TE free turbine speed based on a neural network (fig. 3) has one caveat: although the neural network controller finds a minimum, this minimum is only a local minimum and it cannot be argued that this is the optimal solution. To avoid choosing a suboptimal local minimum in the objective function, it is required to repeat the optimization process several times and choose the best result. It is possible that by setting different initial values of the PID-controller parameters, different optimal controller parameters will be obtained. In addition, during the training of the neural network, several random perturbations are used during each cycle and the reaction time of the system is taken into account to calculate the objective function and its gradient. This ensures obtaining local optimal coefficients of the PID-controller for various disturbances affecting the system. In addition, by changing the step size and the number of perturbations, the sensitivity of the results increases during the search process for the controller coefficients. The process of searching for controller parameters is terminated when a steady state of the system is determined, which is achieved through the calculation of a linear regression of the most recent estimates and iteration until the step response reaches a steady state value with an error of 1 % (fig. 8).

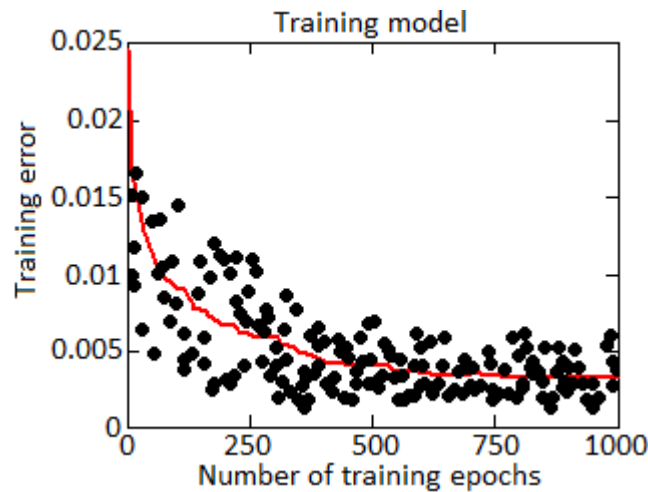


Figure 8: Diagram of the dependence of the objective function on the number of iterations

It should be noted that the adequacy of the model represented by the neural network directly depends on the training process. There are a number of parameters that affect the quality of training: training rate coefficient (assumed 1.5); number of neurons in the hidden layer (assumed 20); length of the delay line of input signals (5 is accepted); number of completed training epochs (assuming 1000 training epochs).

As a criterion for assessing the quality of training, you can use the final total standard deviation for the epoch, which is determined according to the expression:

$$E_{epoch} = \sqrt{\frac{1}{M} \sum_{i=1}^M \left(\frac{1}{2} \sum_{k=1}^m (y_{k out} - y_k)^2 \right)}; \quad (44)$$

where M – number of training sample elements. The training of the neural network continues until one of the stopping criteria is met. For example, the training time will not run out, a certain number of training epochs will pass, or the error per epoch will not exceed the minimum required threshold.

Let's carry out a number of additional research that determine the influence of training parameters on the quality of the neural network, namely:

1. Influence of the training rate coefficient.
2. Influence of the number of neurons in the hidden layer.
3. Influence of the delay length of input signals.
4. Influence of the number of training epochs passed.

The results of the research are given in table 3–6 and in fig. 9, where: a – diagram that determines the influence of the training rate on the final standard deviation; b – diagram that determines the effect of the number of hidden neurons on the final standard deviation; c – diagram that determines the influence of the length of the delay line on the final standard deviation; d – diagram that determines the effect of the number of epochs passed on the final standard deviation.

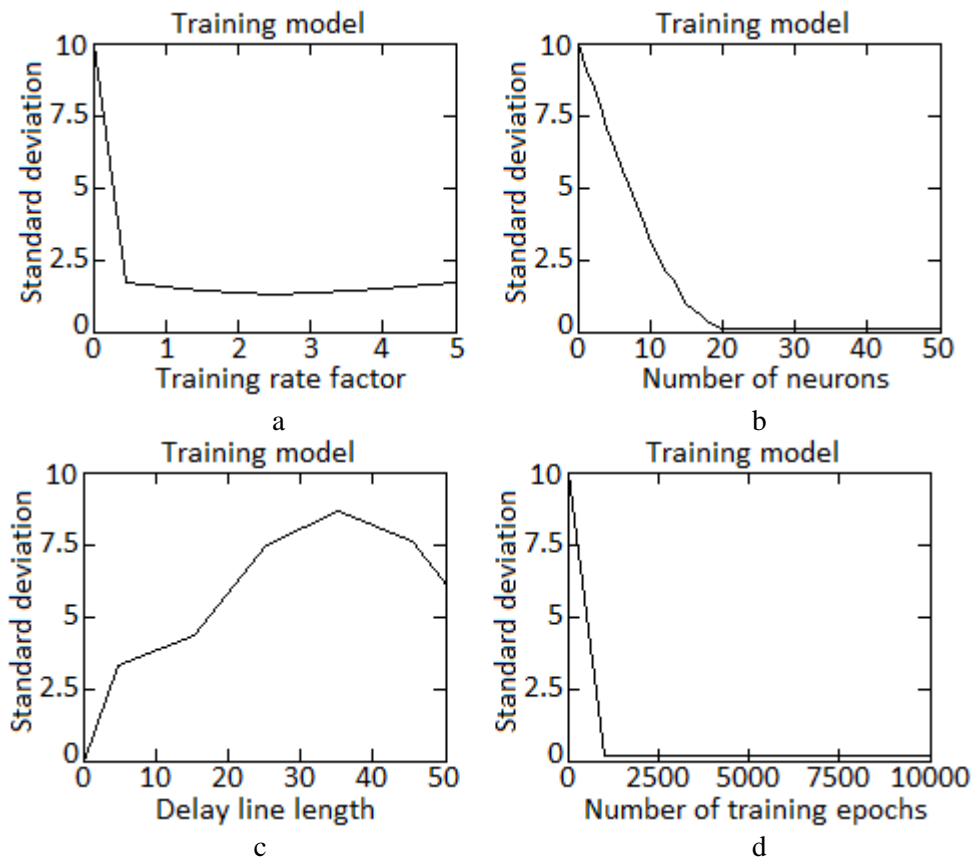


Figure 9: Research results that determine the impact of training parameters on the quality of a neural network

Table 3

Influence of the training rate coefficient on the resulting error

Training rate coefficient	Final standard deviation
0.4	1.722
1.5	1.471
3.6	1.471
5.0	1.723

Table 4

Influence of the number of neurons in the hidden layer on the resulting error

Number of neurons in the hidden layer	Final standard deviation
5	6.360
10	3.138
15	1.004
20	0.126
25	0.126
50	0.126

Table 5

Influence of delay line length on the resulting error

Delay line length	Final standard deviation
0.5	3.349
1.5	4.354
25.1	7.512
50.1	6.029

Table 6

Influence of the number of epochs passed on the resulting error

Epoch of training passed	Final standard deviation
0	10.0
1000	0.239
2500	0.239
5000	0.239
10000	0.239

The conducted studies, which determine the influence of training parameters on the quality of the neural network, allow us to preliminarily state:

1. At low values of the training rate coefficient, slow convergence is observed and there is a risk of hitting a local minimum, while at the same time, the accuracy of hitting an extremum point increases. With large values, it is impossible to achieve a small error, since each step we skip past the extremum.

2. A larger number of neurons in the hidden layer allows you to more accurately describe the training sample at the cost of computing power. At the same time, there is a danger of overfitting when the neural network reproduces noises and distortions in the training sample and is not able to adequately represent the circuit for maintaining the speed of the free turbine of helicopters TE.

3. A large length of the delay line increases the number of input neurons and, consequently, the computational load. At the same time, a longer delay line describes the dynamic properties of the object better and avoids contradictions in training, when the object can change its behavior depending on past influences.

4. The final error depends logarithmically on the number of epochs passed, as a result of which it is not rational to use a large number of epochs, since the computation time increases exponentially and there is a risk of retraining the neural network.

5. Results

Fig. 10 shows the characteristics of the transient process in terms of free turbine frequency rotation according to [13, 14], as well as according to the developed neural network, while:

1) a – diagram of the transient process in terms of the free turbine speed when the engine is operating at flight mode with a linear PD-controller of the circuit for maintaining the free turbine speed;

2) b – diagram of the transient process in terms of the free turbine speed during the operation of a linear PD-controller and a PD-controller with a reduced proportional gain (1 – linear PD-controller; 2 – PD-controller with reduced k_d);

3) c – diagram of the transient process for the speed of the free turbine during the operation of a linear PD-controller and a quadratic controller (1 – linear PD-controller; 2 – quadratic controller);

4) d – diagram of the transient process in terms of the free turbine speed during the operation of a linear PD-controller and a PD-controller with a variable amplification factor (1 – linear PD controller; 2 – PD-controller with a variable amplification factor);

5) e – diagram of the transient process in terms of the free turbine speed during the operation of a linear PD-controller and a fuzzy P-controller (1 – linear PD-controller; 2 – fuzzy logical P-controller);

6) f – diagram of the transient process in terms of the free turbine speed during the operation of a linear PD-controller and a fuzzy P-controller with a corrective differential link (1 – linear PD-controller; 2 – fuzzy logical P-controller with a corrective differential link);

7) g – diagram of the transient process for the free turbine speed during the operation of a linear PD-controller and a neural network PID-controller (1 – linear PD-controller; 2 – PID-controller developed on the basis of a neural network).

Fig. 11 shows diagrams of changes in the values of the coefficients of the PID-controller during the transient process. As follows from fig. 11, the transient process turns out to be very close to the reference process, and the PID-controller with a neural network provides a much higher quality of control than PD-controllers of various architectures (fig. 10, a – f).

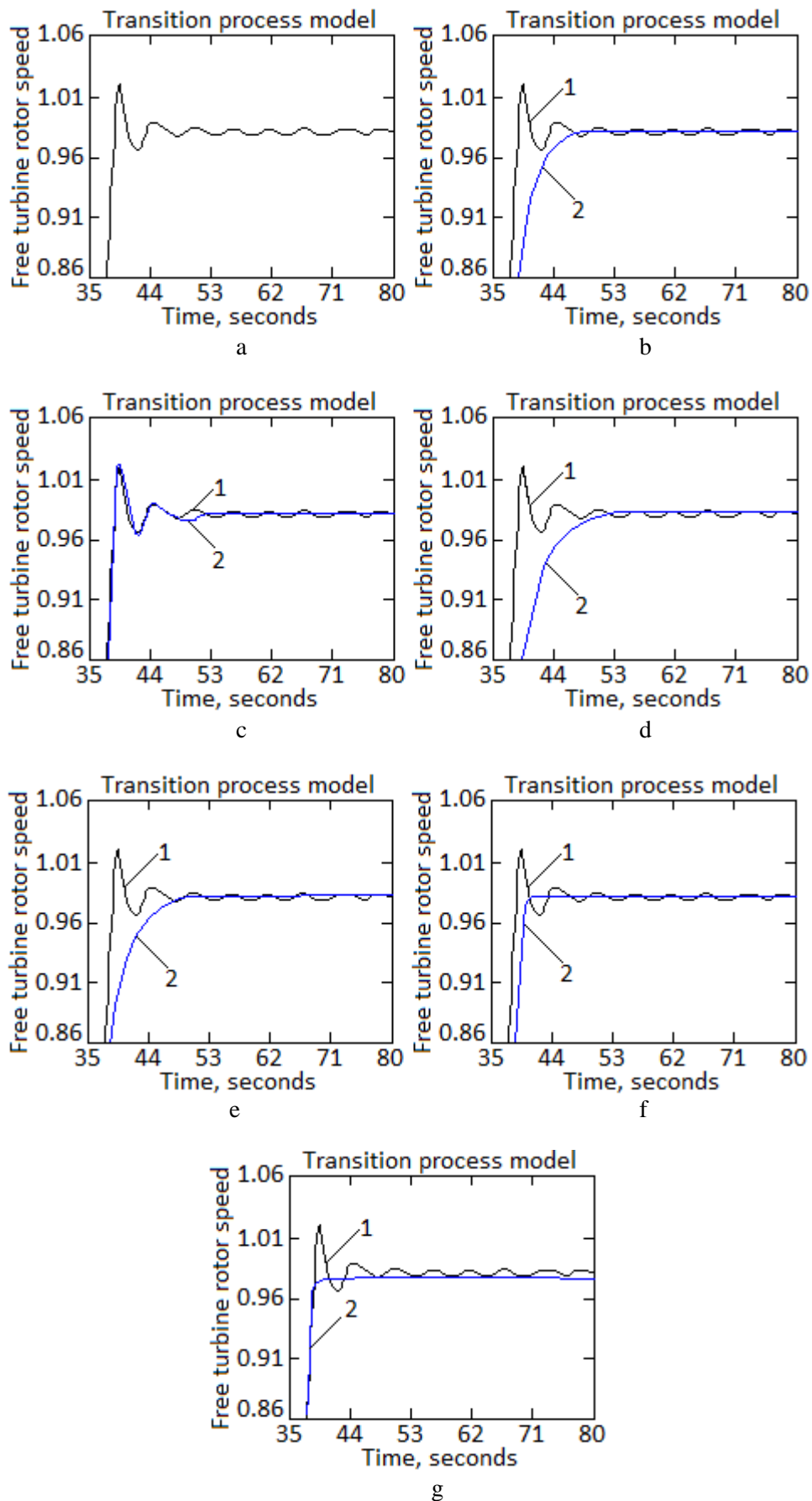


Figure 10: Free turbine frequency rotation transient's processes resulting diagram

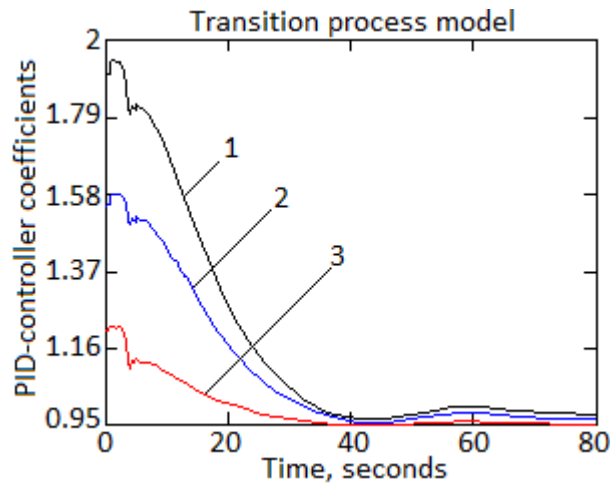


Figure 11: Diagram of the change in the coefficients of the PID-controller during the transient: 1 – k_p ; 2 – k_d ; 3 – k_i

6. Discussions

A comparison was made of the quality of control of the transient response by free turbine frequency rotation and the stability margins provided by each of the considered controllers (Fig. 10). Fig. 12 shows a diagram of the joint arrangement of the transient curves according to the free turbine speed during the operation of various controllers: 1 – linear PD-controller; 2 – PD-controller with reduced k_d ; 3 – quadratic controller; 4 – PD-controller with a variable amplification factor; 5 – fuzzy logical P-controller; 6 – fuzzy logical P-controller with a corrective differential link; 7 – PID-controller developed on the basis of a neural network. Table 7 presents a numerical analysis of the quality of operation of the circuit for maintaining the free turbine speed with various controllers.

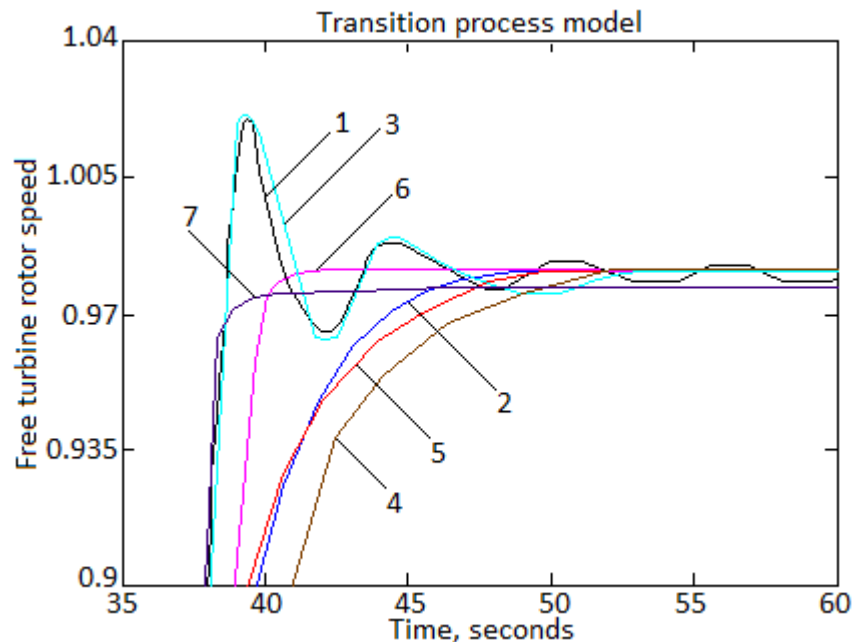


Figure 12: Characteristics of transient processes by the frequency of rotation of the free turbine during the operation of various controllers

Table 7

Analysis of the quality of operation of the circuit for maintaining the free turbine rotation frequency with various controllers

Controller type	Static accuracy, %	Speed, seconds	Transition process nature	Throw value, %
Linear PD-controller	± 0.2	20.0	oscillatory	1.9
PD-controller with reduced k_d	± 0.3	15.0	aperiodic	–
Quadratic controller	± 0.2	18.0	oscillatory	2.2
PD-controller with a variable amplification factor	± 0.2	16.5	aperiodic	0.1
Fuzzy logical P-controller	± 0.1	16.5	aperiodic	–
Fuzzy logical P-controller with a corrective differential link	± 0.2	6.0	aperiodic	0.3
PID-controller developed on the basis of a neural network	± 0.05	3.5	aperiodic	–

From fig. 12 and table 7 it follows that the best quality of the transient process in terms of the free turbine speed is provided by the PID-controller developed on the basis of a neural network. The transient response during operation of this controller differs from others in its higher speed (about 3.5 seconds) and the absence of oscillations (curve 7). The remaining controllers are inferior in terms of providing the required quality of control. According to [13, 14], the transient response in terms of free turbine rotational speed, obtained with the operation of a quadratic controller, does not differ in quality from the characteristic obtained with the operation of the original linear PD-controller (curves 1 and 3). The process is characterized by the presence of fluctuations and overshoot of about 4 %. The oscillation amplitude is 0.2 %. The transition process time is about 20 seconds. When analyzing the characteristics of transients obtained during the operation of a PD-controller with a reduced proportional gain, a variable gain controller, and a P-type fuzzy logic controller, it can be seen that these characteristics differ slightly from each other. The transient process has an aperiodic character (curves 2, 4, 5 and 6) and almost the same speed (for curve 2, the transition process time is 15 seconds, for curves 4, 5 – 16.5 seconds, for curve 6 – 6 seconds).

A comparative analysis of the accuracy provided by each of the considered controllers (Fig. 12) is given in table 8, which shows the probabilities of errors of the 1st and 2nd kind in determining the optimal parameter n_{FT} .

Table 8

The results of determining the probability of errors of the 1st and 2nd kind

Controller type	Probability of error in determining	
	Type 1st error	Type 2nd error
Linear PD-controller	1.95	1.42
PD-controller with reduced k_d	1.74	1.21
Quadratic controller	1.46	1.03
PD-controller with a variable amplification factor	1.32	0.95
Fuzzy logical P-controller	1.08	0.77
Fuzzy logical P-controller with a corrective differential link	0.97	0.64
PID-controller developed on the basis of a neural network	0.58	0.22

As can be seen from table 8, the use of a PID-controller developed on the basis of a neural network provides an improvement in the probability of errors of the 1st and 2nd kind compared to the controllers developed in [13, 14] by 35...85 %.

7. Conclusions

1. The method of maintaining the helicopter rotor speed has been further developed, which, through the use of a PID-controller developed on the basis of a dynamic neural network of direct data transmission based on neurons with a radial basis activation function in the first layer and adalines – neurons with a linear activation function, in the second layer, made it possible to improve the quality of the transient process in terms of helicopter aircraft turboshaft engine free turbine rotation frequency, which consists in increasing the speed up to 3 seconds, increasing the statistical accuracy up to ± 0.05 % and eliminating the overshoot of parameters.

2. The circuit for maintaining the helicopter aircraft turboshaft engine free turbine speed has been improved, which, due to the use of a PID-controller with neural network tuning of the gain factors, made it possible to automatically adjust the amplification factor and, thereby, reduce the time of the transition process.

3. The neural network training method based on the method of programmatic gain adjustment, developed by Professor Volodymyr Zubov, was further developed, which, by integrating direct data transmission into a dynamic neural network based on neurons with a radial-basis activation function in the first layer and adalines – neurons with a linear activation function, in the second layer, made it possible to reduce the error of its training for the problem of researching the transient process in terms of helicopter aircraft turboshaft engine free turbine rotation frequency to 0.005 %.

4. The structure of the PID-controller with an auto-tuning unit based on a neural network has been improved, in which, due to the use of a dynamic neural network of direct data transmission based on neurons with a radial basis activation function in the first layer and adalines – neurons with a linear activation function, in the second layer, as a functional converter that generates the desired amplification factor of the PID-controller for a set of input and output signals, made it possible to improve the probability of errors of the 1st and 2nd kind in comparison with the known controllers by 35 ... 85 %.

8. References

- [1] S. Nandy, R. Singh, A. Maity, P.S.V. Nataraj, Robustification of Unscented Kalman Filtering to Identify Faults in Gas Turbine Engine, *IFAC-PapersOnLine*, vol. 5, issue 1 (2022) 826–831. doi: 10.1016/j.ifacol.2022.04.135
- [2] S. Kim, A new performance adaptation method for aero gas turbine engines based on large amounts of measured data, *Energy*, vol. 221 (2021) 119863. doi: 10.1016/j.energy.2021.119863
- [3] S. K. Valluru, M. Singh, Performance investigations of APSO tuned linear and nonlinear PID controllers for a nonlinear dynamical system, *Journal of Electrical Systems and Information Technology*, vol. 5, issue 3 (2018) 442–452. doi: 10.1016/j.jesit.2018.02.001
- [4] T. Shuprajhaa, S. K. Sujit, K. Srinivasan, Reinforcement learning based adaptive PID controller design for control of linear/nonlinear unstable processes, *Applied Soft Computing*, vol. 128 (2022) 109450. doi: 10.1016/j.asoc.2022.109450
- [5] M. H. Suid, M. A. Ahmad, Optimal tuning of sigmoid PID controller using Nonlinear Sine Cosine Algorithm for the Automatic Voltage Regulator system, *ISA Transactions*, vol. 128, part B (2022) 265–286. doi: 10.1016/j.isatra.2021.11.037
- [6] S. Chen, T. Chen, J. Chu, C. Xu, Global stabilization of uncertain nonlinear systems via fractional-order PID, *Communications in Nonlinear Science and Numerical Simulation*, vol. 116 (2023) 106838. doi: 10.1016/j.cnsns.2022.106838
- [7] M. J. Mahmoodabadi, H. Jahanshahi, Multi-objective optimized fuzzy-PID controllers for fourth order nonlinear systems, *Engineering Science and Technology, an International Journal*, vol. 19, issue 2 (2016) 1084–1098. doi: 10.1016/j.jestch.2016.01.010
- [8] M. Praharaj, D. Sain, B. M. Mohan, Development, experimental validation, and comparison of interval type-2 Mamdani fuzzy PID controllers with different footprints of uncertainty, *Information Sciences*, vol. 601 (2022) 374–402. doi: 10.1016/j.ins.2022.03.095
- [9] M. W. Hasan, N. H. Abbas, Disturbance Rejection for Underwater robotic vehicle based on adaptive fuzzy with nonlinear PID controller, *ISA Transactions*, vol. 130 (2022) 360–376. doi: 10.1016/j.isatra.2022.03.020

- [10] Q. Shi, H.-K. Lam, C. Xuan, M. Chen, Adaptive neuro-fuzzy PID controller based on twin delayed deep deterministic policy gradient algorithm, *Neurocomputing*, vol. 402 (2020) 183–194. doi: 10.1016/j.neucom.2020.03.063
- [11] M. Praharaj, D. Sain, B. M. Mohan, Modelling and analysis of an interval type-2 Mamdani fuzzy PID controller, *IFAC-PapersOnLine*, vol. 55, issue 1 (2022) 728–733. doi: 10.1016/j.ifacol.2022.04.119
- [12] M. Najariyan, Y. Zhao, Granular fuzzy PID controller, *Expert Systems with Applications*, vol. 167 (2021) 114182. doi: 10.1016/j.eswa.2020.114182
- [13] E. Chicherova, Methods for Improvement of the Quality of the Power Turbine Speed Control of a Gas Turbine Engine, *Mechatronics, Automation, Control*, vol. 16, no. 6 (2015) 402–408.
- [14] E. Chicherova, V. Blokhin, S. Konashkov, The use of mathematical models for the development and refinement of the electronic part of the aircraft engine control system, *Science and technology*, vol. 4 (2015) 43–54.
- [15] I. Petukhov, T. Mikhaylenko, S. Yepifanov, O. Shevchuk, Study on accuracy of heat transfer coefficient determination in the bearing chamber for gas turbine, *Proceedings of ASME Turbo Expo 2020 Turbomachinery Technical Conference and Exposition*, G2020-14304.
- [16] I. Danilov, A. Marusin, M. Mikhlik, I. Uspensky, Development of the mathematical model of fuel equipment and justification for diagnosing diesel engines by injector needle displacement, *Transport Problems*, vol. 15, no. 1 (2020) 93–104. doi: 10.21307/tp-2020-009
- [17] I. Oganyan, Mathematical model of fuel pump-regulator of helicopter turbo-shaft engine, *Aerospace Technic and Technology*, no. 17 (167) (2020) 105–112. doi: 10.32620/akt.2020.7.15
- [18] Y. Zhao, B. Niu, G. Zong, N. Xu, A. M. Ahmad, Event-triggered optimal decentralized control for stochastic interconnected nonlinear systems via adaptive dynamic programming, *Neurocomputing*, vol. 529 (2023) 126163. doi: 10.1016/j.neucom.2023.03.024
- [19] Z.-X. Fan, A. C. Adhikary, S. Li, R. Liu, Disturbance observer based inverse optimal control for a class of nonlinear systems, *Neurocomputing*, vol. 500 (2022) 821–831. doi: 10.1016/j.neucom.2022.05.115
- [20] D. Shanin, V. Chikin, Neural network adaptive controller for the problem of controlling an object with an unknown structure by means of global feedback, *Computer and Information Sciences*, no. 4 (2018) 210–218.
- [21] A. Pomogaev, D. Dementev, D. Krasnenko, A. Shtylenko, Exploring the possibility of applying different neuronal activation functions to a single-circuit ACS, *Journal of Physics: Conference Series*, vol. 1889 (2021) 022007. doi: 10.1088/1742-6596/1889/2/022007
- [22] S. Vladov, Y. Shmelov, R. Yakovliev, Modified Helicopters Turboshift Engines Neural Network On-board Automatic Control System Using the Adaptive Control Method. ITTAP'2022: 2nd International Workshop on Information Technologies: Theoretical and Applied Problems, November 22–24, 2022, Ternopil, Ukraine. *CEUR Workshop Proceedings (ISSN 1613-0073)*, vol. 3309 (2022) 205–229.
- [23] S. Vladov, Y. Shmelov, R. Yakovliev, Methodology for Control of Helicopters Aircraft Engines Technical State in Flight Modes Using Neural Networks, *The Fifth International Workshop on Computer Modeling and Intelligent Systems (CMIS-2022)*, May, 12, 2022, Zaporizhzhia, Ukraine, *CEUR Workshop Proceedings (ISSN 1613-0073)* vol. 3137 (2022) 108–125. doi: 10.32782/cmisis/3137-10
- [24] R. Wang, B. C. M. Fung, Y. Zhu, Heterogeneous data release for cluster analysis with differential privacy, *Knowledge-Based Systems*, vol. 201–202 (2020) 106047. doi: 10.1016/j.knsys.2020.106047
- [25] H.-Y. Kim, Statistical notes for clinical researchers: Chi-squared test and Fisher's exact test, *Restor Dent Endod*, vol. 42, no. 2 (2017) 152–155. doi: 10.5395/rde.2017.42.2.152